JOM, Vol. 66, No. 8, 2014
DOI: 10.1007/s11837-014-1016-x

Boron Undoped and Doped Europium-Bismuth Oxide Nanocomposites via the Polymeric Precursor Technique

ARDA AYTIMUR,[1] SERHAT KOÇYIĞIT,[1,3] SINAN TEMEL,[2] and IBRAHIM USLU[1]

1.—Department of Advanced Technologies, Institute of Science, Gazi University, Teknikokullar, 06500 Ankara, Turkey. 2.—Central Laboratory, Bilecik Şeyh Edebali University, Gülümbe, 11210 Bilecik, Turkey. 3.—e-mail: sergas_29@hotmail.com

Boron-undoped and -doped europium-bismuth oxide nanocomposites were synthesized by the polymeric precursor technique. The solutions were calcined and sintered to prepare nanocomposite powders. The nanocomposites were characterized by the Fourier transform infrared spectroscopy, x-ray diffraction, scanning electron microscope, and Brauner–Emmett–Teller techniques. According to Fourier transform infrared spectroscopy results, the shape, the range, and the intensity of the peaks for the calcined and sintered samples changed with the addition of boron content. Furthermore, the reaction path, resulting crystal size, and crystal morphology were all altered by boron additions. A decrease in porosity, brought about by boron additions, also altered the N_2 absorption/desorption characteristics.

INTRODUCTION

Materials based on Bi_2O_3 doped with rare-earth elements such as europium have important electrical, magnetic, and optical properties that make them suitable for important applications such as solid oxide fuel cell (SOFC) technology, thermal and mechanical sensors, scintillation counters, and many kinds of optical devices.[1–3] Europium is different from many of the rare-earth ions because it can have two different valence states (2+ and 3+),[4,5] which are responsible for many of the technologically relevant material behaviors.[3]

Boron is another important dopant addition to Bi_2O_3 that is used to control the ratio of octahedral-BiO_6 and pyramidal-BiO_3 structural units.[6,7] Using boric acid source material has the additional advantages of being nontoxic and inexpensive.[8] Boron-doped europium-bismuth oxide can be synthesized by a variety of techniques including powder mixing, milling, and the polymeric precursor technique (PPT). The method of preparation is an important consideration because the size and morphology of the resulting crystals can cause property changes as compared with an individual crystal. In this study, PPT was preferred because PPT is the best method for controlled formation of nanostructures. By employing metal acetate precursors, such as europium acetate in polyvinyl alcohol (PVA), the molecular homogeneity of the precursors is accurately maintained.[9,10]

The aim of this study is to prepare boron-doped europium-bismuth oxide nanocomposite ceramics by calcination, sintering, and removal of the organic structures of PVA/boron-undoped and -doped bismuth-europium acetate hybrid polymer solutions. In addition, we characterize and comment on the crystal and morphological structures that result from the subsequent phase transitions.

EXPERIMENTAL PROCEDURE

Polyvinyl alcohol (PVA-Mw 85,000-124,000 g/mol, Sigma-Aldrich) was used as the polymeric precursor. Europium (III) acetate hydrate (99.99%, Sigma-Aldrich), bismuth (III) acetate (99.99%, Sigma-Aldrich), boric acid (99.97% Sigma-Aldrich), and PVA (Sigma-Aldrich, Mw: 85000–124000) were used as starting materials. Ultrapure deionized water and acetic acid (100%, Merck) were used as the solvent.

PVA solution (10%, w/w) was produced by dissolving PVA powder into ultrapure water; then the solution was slowly heated to 80°C over 2 h and cooled back to room temperature. For the undoped solution, 1.5000 g of bismuth(III) acetate and 0.3249 g of europium acetate hydrate were then

(Published online June 17, 2014)

added. For the boron-doped solution, an additional 0.2189 g of boric acid was added to the 20 g of aqueous PVA at room temperature and stirred vigorously for 3 h at room temperature. Thus, sol-gels of boron-undoped and -doped PVA/Bi-Eu acetate hybrid polymer solutions were obtained. Calcination was performed by heating the solutions in air at a rate of 8°C/min with an isothermal hold at 850°C for 2 h; the calcined powders were sintered in air by heating to 1000°C at 8°C/min and holding for 3 h.

The pH and conductivity of the polymer solutions were measured using a pH 315i meter and conductivity meter (Wissenschaftlich-Technische Werkstätten (WTW) GmbH & Co. KG). The viscosity of the solutions was determined using a SV-10 viscometer. Surface tension measurements were performed using a KRUSS manual measuring system.

The crystal structure was carefully examined by x-ray diffraction (XRD) and Fourier transform infrared spectroscopy (FT-IR). X-ray powder diffraction patterns of nanocomposite powders were collected using a PANalytical Empyrean x-ray diffractometer using Cu Kα radiation (λ = 1.54 Å). FTIR spectra (4000–380 cm^{-1}) were recorded on a Perkin-Elmer Spectrum 100 FTIR spectrometer and by ATR (with a diamond-protected attenuated total reflectance crystal unit) at a resolution of 4 cm^{-1}after 100 scans.

The microstructures of these samples were observed using scanning electron microscopy (Field Emission SEM ZEISS, SUPRA 40 VP) on samples sputtered with platinum (Qourum Q 150R ES DC Sputter) and observed at an accelerating voltage of 10 kV. The surface area and porosity of the nanocomposite powders were analyzed using the Burnauer, Emmett, and Teller (BET) technique (Asap 2020, Micromeritics).

RESULTS AND DISCUSSION

The values of viscosity, surface tension, pH, and electrical conductivity of the complex hybrid polymer solutions were measured and given in Table I for both samples before the calcination and sintering procedures. As was expected, the addition of boron resulted in an increase in the viscosity and surface tension but in a decrease in the pH.

In Figs. 1 and 2, the FT-IR spectra can be compared for the undoped and doped conditions, respectively, in their (a) calcined and (b) sintered states. The bands in Fig. 1a at 626 cm^{-1}, 530 cm^{-1}, 497 cm^{-1}, and 466 cm^{-1} are related to the vibrational peaks between bismuth and oxygen bonds in BiO_6 octahedral units.[11,12] Likewise, the characteristic vibrational peaks between bismuth and oxygen bonds in BiO_3 also give infrared bands at 466 cm^{-1}, 530 cm^{-1}, 626 cm^{-1}, and 842 cm^{-1}. The peak at 711 cm^{-1} is related to the stretching vibrational

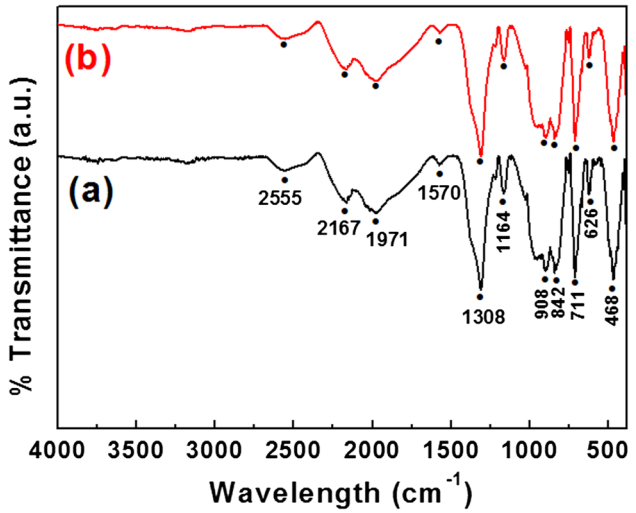

Fig. 1. The FT-IR graphs of Eu/Bi oxide calcined (a) and sintered (b) nanocomposite powders for boron-undoped nanocomposite powder.

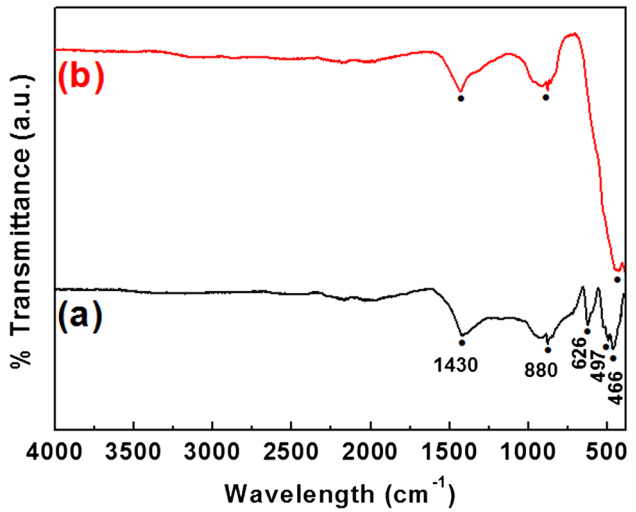

Fig. 2. The FT-IR graphs of Eu/Bi oxide calcined (a) and sintered (b) nanocomposite powders for boron-doped nanocomposite powder.

Table I. Viscosity, surface tension, ph, and electrical conductivity of the complex hybrid polymer solutions for boron-undoped (Sol-1) and -doped (Sol-2) samples

Solution #	pH	Electrical conductivity (mS/cm)	Viscosity (mPa s)	Surface tension (mN/m)
Sol-1	2.56	1.53	88.4	52
Sol-2	2.48	1.53	122	53

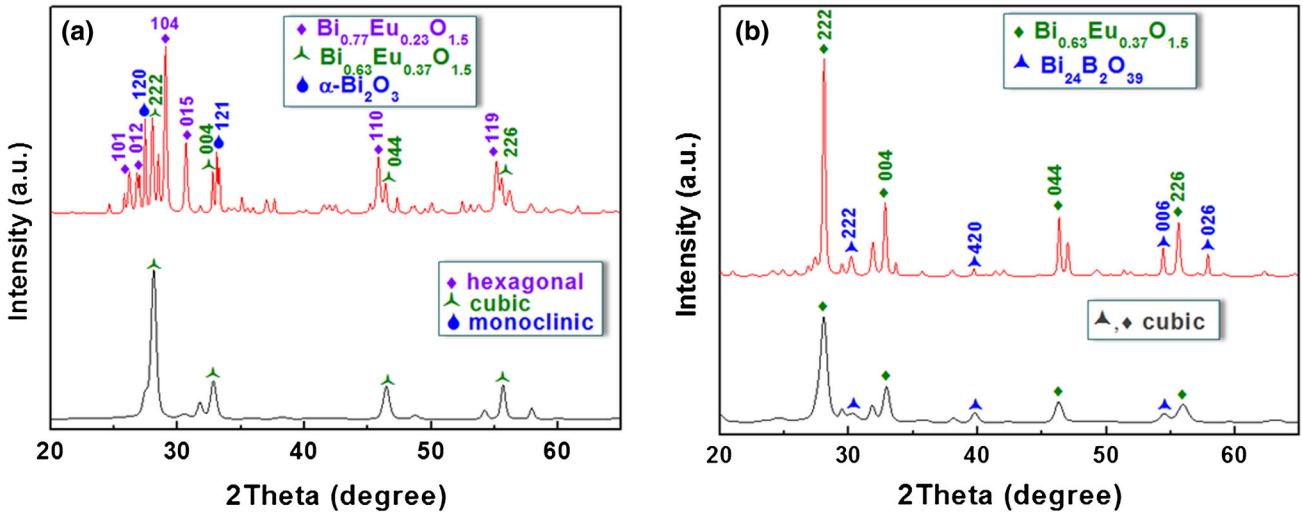

Fig. 3. X-ray diffraction graphs of calcined (black trace) and sintered (red trace) boron-undoped (a) and -doped (b) europium-bismuth oxide nanocomposite powder (Color figure online).

Table II. Calculated lattice parameters of boron-undoped calcined (undoped-1) and sintered (undoped-2) and of boron-doped calcined (doped-1) and sintered (doped-2) nanocomposite powders via Scherrer equation

Sample	(*hkl*)	2*θ* (°)	FWHM (°)	*d* (Å)	*a* = *b* (Å)	*c* (Å)
Undoped-1	(222)	28.12	0.4680	3.17	10.98	10.99
Undoped-2	(222)	28.03	0.2184	3.18	11.02	11.02
	(104)	29.07	0.2184	3.07	3.97	27.31
Doped-1	(222)	28.09	0.2496	3.17	10.99	10.99
Doped-2	(222)	28.07	0.6084	3.18	11.00	11.00

peaks between bismuth and oxygen bonds in BiO_3 units[13] as can be seen in both Figs. 1 and 2. For the sintered samples, some of the Bi-O bonds in BiO_6 octahedral units are not present in the calcined nanocomposite powders. Vibrational spectra of Bi_2O_3 and derivatives studied by infrared spectroscopy indicated that bismuth does not form a simple structure; however, it is well known that bismuth ions can form [BiO_3] pyramidal or [BiO_6] octahedral units. The presented bands in the FTIR spectra of the samples confirm the formation of Bi_2O_3 with a structure based on BiO_6 and BiO_3 units. The shape, range, and intensity of the peaks for the calcined and sintered samples changed with the addition of boron content indicating the contribution of the vibrations between boron and oxygen bonds.

X-ray diffraction patterns of the calcined (black trace) and sintered (red trace) boron-undoped (a) and -doped (b) europium-bismuth oxide nanocomposite ceramic powders are shown in Fig. 3. According to the JCPDS card, one body-centered-cubic (bcc) phase (Ref. No: 98-008-0403) is present in the calcined boron-undoped sample. Two additional phase types have been identified in Fig. 3 as bcc $Bi_{0.63}Eu_{0.37}O_{1.5}$ (Ref. No: 98-008-0403), hexagonal $Bi_{0.77}Eu_{0.23}O_{1.5}$ (98-009-4229), and monoclinic α-Bi_2O_3 (98-005-0641). The boron-doped sample in its calcined state, given in Fig. 3b, includes two cubic phases and does not undergo a significant phase change, but instead significant peak sharpening is observed. The most important changes in the reaction path are a lack of the hexagonal $Bi_{0.77}Eu_{0.23}O_{1.5}$ and the α-Bi_2O_3 phases in the final structure of the sintered boron-doped sample.

According to the XRD results, the lattice parameters (a and d) of the nanocomposite powders were calculated using the following equations:[14]

$$\frac{1}{d^2} = \frac{h^2 + k^2 + l^2}{a^2} \tag{1}$$

$$\frac{1}{d^2} = \frac{4}{3}\left(\frac{h^2 + hk + k^2}{a^2}\right) + \frac{l^2}{c^2} \tag{2}$$

Equation 1 is used in cubic phase, and Eq. 2 is used in hexagonal phase. The calculated lattice constants (a) of the boron-undoped and -doped stabilized europium-bismuth oxide nanocomposite powders are given in Table II, respectively.

Figure 4 shows an SEM micrograph of undoped (a, b) calcined and (c) sintered Eu/Bi powders. Figure 4b shows a sintered sample. Figure 4b is a higher magnification image of Fig. 4a that reveals the nano-

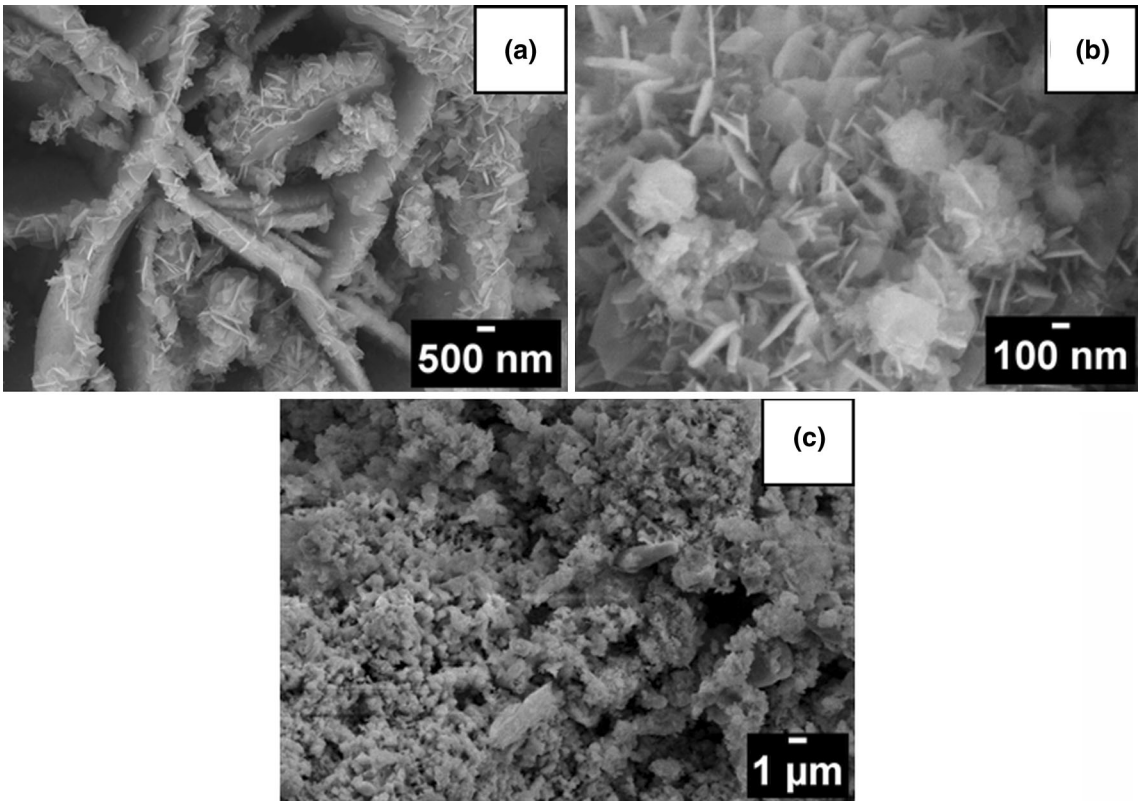

Fig. 4. The SEM micrograph of Eu/Bi oxide calcined (a, b) and sintered (c) for boron-undoped nanocomposite powder.

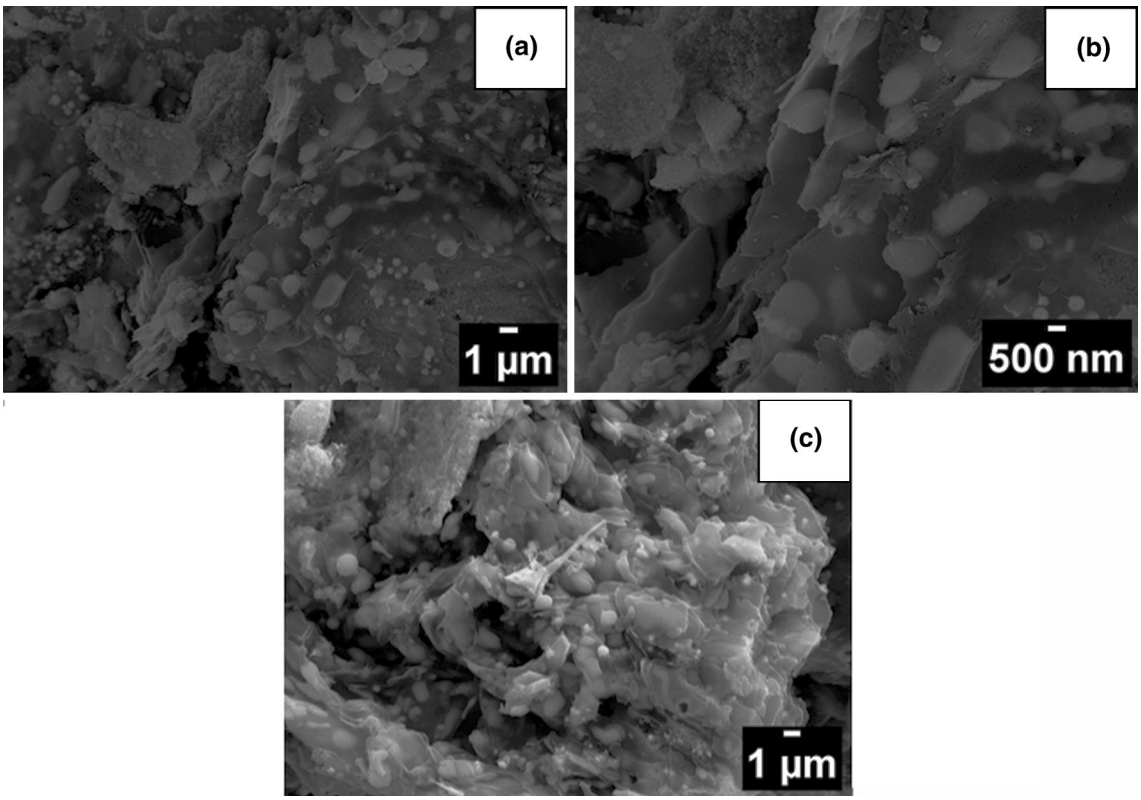

Fig. 5. The SEM micrograph of Eu/Bi oxide calcined (a, b) and sintered (c) for boron-doped nanocomposite powder.

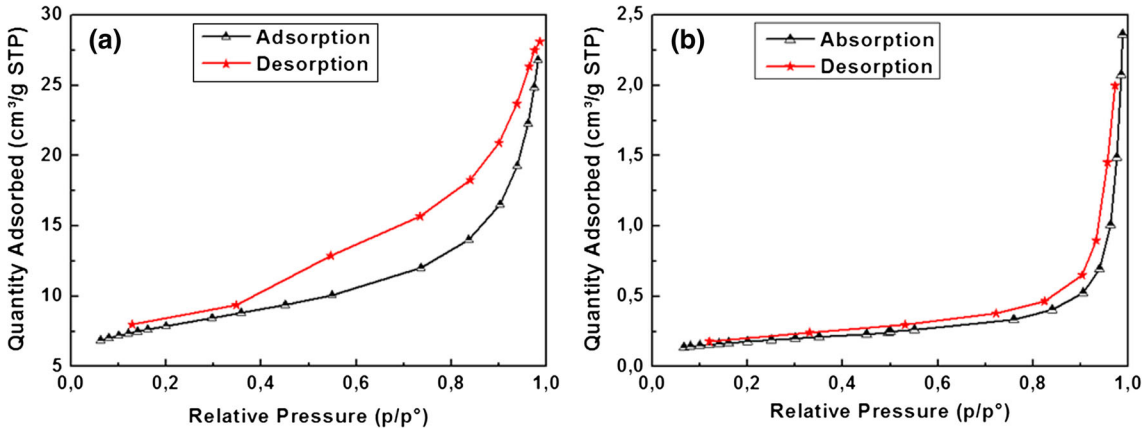

Fig. 6. N_2 adsorption/desorption isotherms of the calcined (a) and sintered (b) boron-undoped nanocrystalline composite powder.

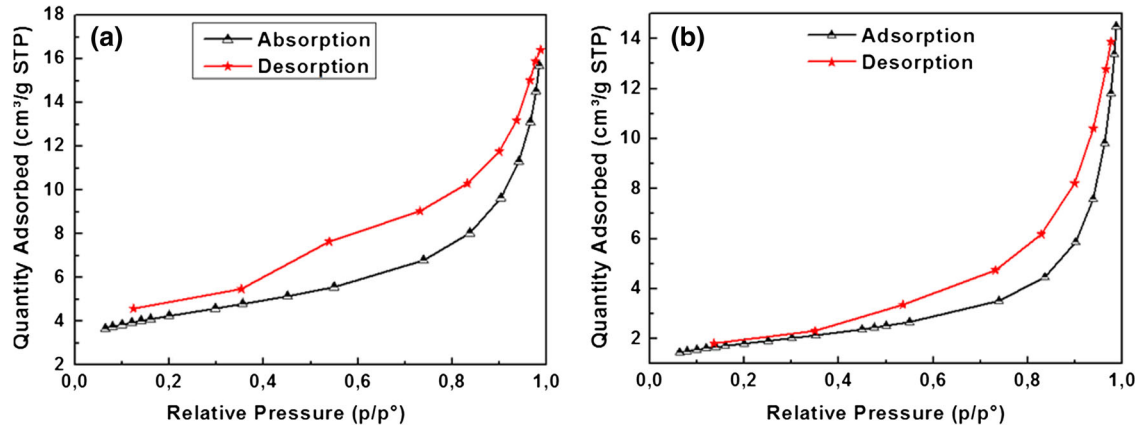

Fig. 7. N_2 adsorption/desorption isotherms of the calcined (a) and sintered (b) boron-doped nanocrystalline composite powder.

structure of the approximately 200-nm-sized, very thin, well-oriented, flower-like nanostructures. During sintering, the sample crystal structure and morphology is altered and results in a sponge-like and porous structure. The mean diameter of the grains is also larger (~600 nm) after sintering.

The microstructure of the boron-doped samples is given in Fig. 5 and shows that the resulting grain morphology is significantly different. Figure 5c shows a higher magnification image that reveals uniformly distributed spherical grains with an average size of 300 nm. Sintering appears to only affect the average diameter without altering the phase makeup or general crystal shape. In general, it is apparent that the doping of Bi_2O_3 nanocomposite has a significant effect on the morphology with respect to the undoped ones of the resultant nanostructure.

The specific surface area of a powder may be determined by BET method. The determination in this method is based on physical adsorption of a gas (usually nitrogen) on the surface of the powder. The amount of adsorbate gas is used in the calculation of the specific surface area according to BET theory.[15] As it is shown in the isotherm figures of the samples (Figs. 6 and 7), there is distinct hysteresis loops at adsorption/desorption isotherms for both samples. Brunauer et al.[15] found that most of the adsorption isotherms fit into one of the five well-known types given in the literature.[16] Both calcined boron-doped and -undoped samples are convex to relative pressure axis and fit into type III groups. The nitrogen adsorption measurements of the two sintered powder samples include the determination of the (I) BET and Langmure surface area and (II) average nanoparticle size. The structural parameters of the sintered powders obtained from BET analysis are presented in Table III. Europium-doped, boron-undoped Bi_2O_3 nanocomposite exhibits a BET surface area of 27.3 m^2/g. Boron doping to the composite decreased the surface areas of the powders by 50% with respect to the undoped ones. The BET surface area of the powders decreased to 14.8 m^2/g. The surface area of undoped powder samples was thus about two times larger than that of the doped one. After sintering both boron-undoped and -doped samples, pore volume decreased and the average particle size of the sintered boron-doped samples also increased by a factor of three times with respect to calcined samples. The decrease of pore volume

Table III. Surface area, pore volume, and pore diameter of the sintered nanocomposite powders

Sample #	BET surface area (m^2/g)	Average nanoparticles size (Å)
Boron undoped (Calcined)	27.3	2196
Boron undoped (Sintered)	0.4	147529
Boron doped (Calcined)	14.8	4056
Boron doped (Sintered)	4.5	13366

after sintering shows a high level of consistency with those obtained by XRD and SEM analysis.

CONCLUSION

Nanocomposites of europium-bismuth oxide were synthesized using the polymeric precursor technique with and without boron doping. Polyvinyl alcohol was used as the polymeric precursor, and boron-undoped and -doped PVA/Eu-Bi hybrid polymer solutions were produced. The viscosity and the electrical conductivity increased, and the pH values decreased with the addition of boron in the solution. Nanocrystalline powders were produced via calcination and sintering processes. According to FT-IR results, the shape, the range, and the intensity of the peaks for the calcined and sintered samples were significant with the addition of boron content. The boron additions also changed the reaction path during the initial calcination process. In addition to the difference in phase selection, the calcination and sintering processes altered the final grain size and morphology significantly. As expected, sintering decreased the BET surface areas of the nanocomposites, but a less porous structure was observed for the boron-doped samples.

REFERENCES

1. F.H. ElBatal, S.Y. Marzouk, N. Nada, and S.M. Desouky, *Phys. B* 391, 88 (2007).
2. P. Pascuta and E. Culea, *Mater. Lett.* 62, 4127 (2008).
3. P. Pascuta, G. Borodi, and E. Culea, *J. Non-Cryst. Solids* 354, 5475 (2008).
4. P. Pascuta, M. Bosca, M. Culea, S. Simon, and E. Culea, *Mod. Phys. Lett. B* 22, 447 (2008).
5. T. Ristoiu and E. Culea, *J. Non-Cryst. Solids* 279, 93 (2001).
6. W.H. Dumbaugh, *Phys. Chem. Glasses* 27, 119 (1986).
7. S. Hazra, S. Mandal, and A. Ghosh, *Phys. Rev. B* 56, 8021 (1997).
8. J.M. Ting, *J. Am. Ceram. Soc.* 77, 2751 (1994).
9. M. Takeyama and C.T. Liu, *Acta Metall. Sin.* 36, 1241 (1988).
10. Z.W. Zhang, C.T. Liu, S. Guo, J.L. Cheng, G. Chen, T. Fujita, M.W. Chen, Y.W. Chung, S. Vaynman, M.E. Fine, and B.A. Chin, *Mater. Sci. Eng. A-Struct.* 528, 855 (2011).
11. V. Dimitrov, Y. Dimitriev, and A. Montenero, *J. Non-Cryst. Solids* 180, 51 (1994).
12. R. Iordanova, Y. Dimitriev, V. Dimitrov, S. Kassabov, and D. Klissurski, *J. Non-Cryst. Solids* 231, 227 (1998).
13. I. Ardelan and D. Rusu, *J. Optoelectron. Adv. Mater.* 10, 66 (2008).
14. C. Suryanarayana and M.G. Norton, *X-ray Diffraction a Practical Approach* (New York, NY: Plenum Press, 1998).
15. S. Brunauer, L.S. Deming, W.S. Deming, and E. Teller, *J. Am. Chem. Soc.* 62, 1723 (1940).
16. N.U. Yagsi, (M.Sc Thesis, Middle East Technical University, 2004).